IEEE Access
Multidisciplinary | Rapid Review | Open Access Journal

Received September 17, 2021, accepted October 15, 2021, date of publication October 22, 2021, date of current version October 28, 2021.

*Digital Object Identifier 10.1109/ACCESS.2021.3122239*

# Optimizing Reconfigurable Manufacturing Systems for Fluctuating Production Volumes: A Simulation-Based Multi-Objective Approach

**CARLOS ALBERTO BARRERA DIAZ[1], TEHSEEN ASLAM[1], AND AMOS H. C. NG[1,2]**
[1]Division of Intelligent Production Systems, School of Engineering Science, University of Skövde, 54128 Skövde, Sweden
[2]Division of Industrial Engineering and Management, Department of Civil and Industrial Engineering, Uppsala University, 75121 Uppsala, Sweden

Corresponding author: Carlos Alberto Barrera Diaz (carlos.alberto.barrera.diaz@his.se)

This work was partially supported by the Knowledge Foundation (KKS), Sweden, through the funding of the research profile Virtual Factories with Knowledge-Driven Optimization (VF-KDO) (2018-2026).

**ABSTRACT** In today's global and volatile market, manufacturing enterprises are subjected to intense global competition, increasingly shortened product lifecycles and increased product customization and tailoring while being pressured to maintain a high degree of cost-efficiency. As a consequence, production organizations are required to introduce more new product models and variants into existing production setups, leading to more frequent ramp-up and ramp-down scenarios when transitioning from an outgoing product to a new one. In order to cope with such as challenge, the setup of the production systems needs to shift towards reconfigurable manufacturing systems (RMS), making production capable of changing its function and capacity according to the product and customer demand. Consequently, this study presents a simulation-based multi-objective optimization approach for system re-configuration of multi-part flow lines subjected to scalable capacities, which addresses the assignment of the tasks to workstations and buffer allocation for simultaneously maximizing throughput and minimizing total buffer capacity to cope with fluctuating production volumes. To this extent, the results from the study demonstrate the benefits that decision-makers could gain, particularly when they face trade-off decisions inherent in today's manufacturing industry by adopting a Simulation-Based Multi-Objective Optimization (SMO) approach.

**INDEX TERMS** Multi-objective optimization, reconfigurable manufacturing systems, simulation-based optimization, genetic algorithm.

## I. INTRODUCTION

In the current competitive manufacturing industry, companies often face a dynamic market wherein fluctuating production volumes need to be addressed to cope with demand variations. How rapidly can a manufacturing system react and adjust its functionalities and capacity according to demand and volume variations encompasses one of the most critical considerations for manufacturing companies [1]–[3]. Reconfigurable Manufacturing Systems (RMS) concept was first introduced by Koren *et al.* [4] as an attempt to address, among others, the challenges derived from such demand and volume fluctuations. RMS are production systems capable of adding, removing, and relocating components, e.g., machines, material handling equipment, etc., to rapidly fulfill expected or unexpected market shifts [5]. Recent studies imply that RMS may be crucial for addressing dynamic production volumes. Therefore, they can help manufacturing companies attain market demands while evading the large investment lost related to non-operating machines [2], [6]. To this extent, RMS are responsive manufacturing systems that provide the capacity and functionality needed for several demand periods by adding or reconfiguring the arrangement of machines and the process plan in a cost-effective manner [1].

RMS consists of several workstations (WSs) where each WS contains several parallels and identical machines [7]. In this study, the RMS configuration is determined by the number of parallel machines and the task sequence to be performed in every WS. The RMS configurations can be classified according to the number of products they produce. Single-part flow line (SPFL) configuration when a single product is produced in the system, and the multi-part flow line (MPFL) configuration when several products are made in the system [8]–[10]. The use of MPFL configurations is

The associate editor coordinating the review of this manuscript and approving it for publication was Jagdish Chand Bansal.

becoming more and more common, especially in the automotive industry where several parts are fabricated in the same flow line [1]. Up to this time, prior studies focused on RMS configuration analysis and task assignment for MPFL are scarce [1], [11], [5]. Furthermore, studies that have treated similar problems, such as the configuration analysis and task assignment for RMS, have set interstation buffers to the same constant capacity, practically ignoring the buffer allocation problem.

Despite the advantages of RMS in handling demand fluctuations and scalable capacities in comparison to traditional manufacturing systems, designing and managing these systems involve complicated and combinatorial NP-hard problems that can be benefited from the use of simulation and optimization techniques [6], [12]–[14]. Due to its betters results in nearing the optimal solutions, metaheuristics methods such as Genetic Algorithms (GAs) have gained attention from many researchers in the field [12]. However, regardless of the successful applications shown by both techniques, studies presented their deficiencies when employed separately. For decades, simulation methods have been successfully employed for modeling and analyzing manufacturing systems [15]. The complex and dynamic scenarios found in manufacturing systems need to be analyzed, assessed, and hence modeled in simulation technology. When a simulation model is built, engineers and decision-makers obtain a better understanding of real-life systems [16]. Simulation, especially Discrete-Event Simulation (DES), is identified as a practical approach to evaluate the uncertainty found in complex manufacturing systems and can consider the changes of the system over time [17]. Nonetheless, as the complexity and the number of variables in the manufacturing system increases, the use of simulation becomes computationally impractical. On the other hand, the use of optimization methods such as metaheuristics can provide solutions to bigger-scale NP-hard problems [12]. Still, in regards to RMS, most of the studies simplified the problem by neglecting the variability of the system and hence producing inaccurate results. To overcome these shortcomings, Simulation-Based Optimization (SBO) emerged to use the benefits of both, i.e., combining the advantages of simulation and optimization. SBO has been proven to be a successful method that leads to improvements in manufacturing systems. Although SBO has been previously used to optimize RMS, the use of Simulation-Based Multi-Objective Optimization (SMO) to deal with the RMS configuration problem and task assignments to WSs is sporadic. Accordingly, researchers identify opportunities in the use of SMO techniques in real-scale RMS problems [6], [18].

Against this backdrop, this study aims at contributing to the RMS research domain by presenting an SMO approach for the optimization of the system configuration of an MPFL subjected to scalable capacities to cope with fluctuating production volumes by addressing the assignment of the tasks to WSs and buffer allocation for maximum throughput (THP) and minimum total buffer capacity (TBC), simultaneously.

The remaining of the paper is organized as follows: In section 2, a literature review of some of the most relevant work in related areas is presented, and its shortcomings are identified. In section 3, the current industrial need to use and optimize RMS to tackle fluctuating production volumes for dynamic market demand is explained. In section 4, the proposed SMO approach is explained. Section 5 shows the proposed approach applied and validated in an industrial-inspired application. Lastly. Section 6 summarizes and concludes this study.

## II. LITERATURE REVIEW

An optimal RMS design needs to address three main areas: the system configuration, the components of the system, and the process planning [5]. The system configuration involves the arrangement of machines in the systems [5]. This has a great impact on the productivity, functionality and scalability aspects of the system [19]. The majority of the research focuses on machine assignment to WSs. The components of the system deal with the type and number of machines or components required to reach the desired production capacity [5]. This is a critical area for capacity planning and scalability. Most of the research concerning this area is devoted to optimizing the number of machines in the system. Lastly, the process planning includes how tasks are allocated to the WS and balanced throughout the system. This area impacts on the reconfiguration efficiency of the system in handling the fluctuating production volumes [20], [21]. Research tends to focus on optimizing the task allocation to WSs. Consequently, during the lifecycle of an RMS, changes in the production are accommodated through one or several reconfigurations. For an RMS to scale the production capacity or deal with demand fluctuations, the system is required to efficiently change its configuration by adding, re-allocating, or removing components and rebalancing the tasks in the reconfigured system [2], [22]. Hence, most of the research on RMS uses a range of different techniques to target one or several aspects related to the mentioned areas. Some of the most relevant studies are listed below.

When it comes to SPFL, Koren and Shpitalni introduced a four steps mathematical approach for determining the number of machines required in a system and selecting the desired RMS configuration to reach the desired production capacity [3]. Another mathematical approach was presented by Wang and Koren in [22] to either maximize the throughput of the system or minimize the number of machines used in the system. In this approach, the authors reconfigure the system and rebalance the task assignment to meet a new production demand in an RMS without buffers. In a later study, Koren, Wang and Gu extended the previous study, including three scenarios in which the in-between buffers have the same constant buffers capacity and defined five design-for-scalability principles. Studies such as [23]–[27] have focused on the cost or profits aspects to find the optimal SPFL configurations. Some other studies, such as [28]–[30], targeted the task assignment and employed a GA to find the

best task allocation for minimal reconfiguration cost or the number of machines.

Contrary to the single-objective above studies, Goyal *et al.* in [9] presented a GA-based approach to obtain the optimal configuration in terms of cost, convertibility, and utilization of machines. Goyal and Jain [31] presented another multi-objective study, using a particle swarm optimization in this case, to find a set of non-dominated SPFL also with convertibility, utilization of machines, and cost as objectives. Another multi-objective, in this case, simulation-based approach, was presented by Barrera-Diaz *et al.* in [15], where NSGA II was employed for the selection of the optimal configuration in terms of maximum production rate, minimum buffer capacity, and minimum lead time. Multi-objective approaches for RMS process plan generation were studied by Khezri *et al.* in [32], targeting sustainability, total production time, and production cost as objectives.

In the case of MPFL, Saxena and Jain used a mathematical approach to minimize RMS configuration design cost [33]. Two linear programming approaches for the configuration design of scalable RMS were illustrated in a hypothetical part family example by Moghaddam *et al.* in [34]. Bortolini *et al.* in [35] presented another linear programming approach for the design of RMS, focusing on part routings with time cost minimization as the objective. Hasan *et al.* present a method in [36] to determine the optimal configuration and part family sequence in an RMS. Youssef and ElMaraghy in [10] used a GA to find the optimal MPFL configuration with minimal cost. Minimal capital cost was again the objective in another GA approach proposed by Dou *et al.* for the MPFL configuration problem in [8]. Dou *et al.* in [1], a multi-objective particle swarm optimization was proposed to address the MPFL configuration problem where minimal cost and tardiness were set as the objectives. Some studies have applied simulation-based methods to solve MPFL process plan generation problems. Musharavati *et al.* in [37] studied the process plan generation in MPFL through a simulated annealing approach. The authors considered a total cost single-objective function. Completion time and cost were the objectives in a study presented by Benyouced and Tiwari [38], where an NSGA II was adopted for the process plan generation in the MPFL. Bensmaine *et al.* [39] studied an SBO approach for the process plan generation of MPFL in which NSGA II is employed to optimize total time and cost. Another SBO approach was studied by Touzout and Benyoucef [40] for process plan generation of an MPFL with three objectives, total time, total cost, and greenhouse gasses emissions. The authors compared the use of three hybrid metaheuristics algorithms.

Regardless of the purpose of the study, e.g., process plan generation or configuration analysis, most of the SPFL or MPFL studies have neglected important aspects such as buffers consideration or system uncertainty and variability. Besides, although SBO has been employed, its use is very sporadic and has either focus on process plan or configuration analysis. None of the reviewed studies have used SBO to combine tasks and resource assignment with system configuration analysis in a scalable MPFL for fluctuating production volumes. This indicates a clear research gap in the use of SMO meta-heuristics techniques to simultaneously address several RMS areas considering optimal buffer capacities as additional decision variables and the unreliability of the machines.

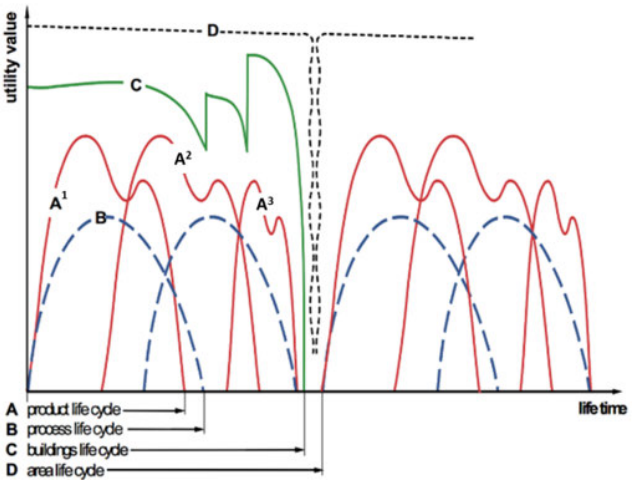


**FIGURE 1.** Shortened lifecycles. Inspired by [42].

## III. INDUSTRIAL NEEDS

Globalization has contributed to bringing the world closer. People around the world are more connected than ever before, information and financial flows are more rapid than ever and products that are manufactured in other parts of the world are seamlessly available to end-users as local products. Nevertheless, this transformation has also contributed to creating a volatile and sometimes unknown landscape for the manufacturing industry. Manufacturing enterprises today are subjected to intense global competition, increasingly shortened product lifecycles and increased product customization and tailoring while being pressured to maintain a high degree of cost-efficiency [41].

The previous stable lifecycles of development and release of new products were characterized by a smooth ramp-up with a steady volume increase which generally was followed by a maturity phase with stable demands and then a smooth ramp-down. In today's global and volatile market, these lifecycles are not only becoming shorter and shorter, but they also display new characteristics, as shown in Fig. 1, where product volumes rise much faster to a first peak following a decrease in demand after a period of time, which is mitigated by promotions campaigns, minor product updates or facelifts increasing the demand to a second peak before a sudden decrease in demand of the product due to announcement of a new product release These lifecycle characteristics are, to a large extent, the results of the end user's requirements of increased customization and personalization of products which is forcing manufacturing industry into a new manufacturing paradigm shift from today's mass customization to mass personalization or individualization [5]. As a

consequence of the shorter product lifecycles and customization, production is required to manufacture an increasing number of product models and variants [42]. It is estimated that product lifecycles have been reduced by 25%, leading to that product variety has more doubled in the last two decades [43].

With the above-said trend, production organizations in the future are most likely required to introduce more new product models and variants into existing production setups, leading to more frequent ramp-up and ramp-down scenarios when transitioning from an outgoing product to a new one. For instance, Fig. 1 depicts the interactions of the product lifecycles of A1, A2 and A3 with overlapping ramp-up and ramp-down period between one product to another. Some industry domains are already today facing even more intersecting product lifecycles where the production organization is required to ramp up both product A2 and A3 over a period of time whilst still ramping down product A1. In order to cope with the higher degree of new product models, the productions system setups need to shift towards RMS, which, as explained in the introduction, provide a higher degree of modularity and reconfigurability, making production capable of changing its function and capacity according to the product and customer demand [44].

The RMS paradigm provides the manufacturing industry and production organizations the ability to quickly adapt to these market and product changes in a cost-effective manner, in which the efficiency of a dedicated manufacturing system with high throughput and the flexibility of a flexible manufacturing system is combined with the capability of adapting to market requirements, both in terms of product and volume [3]. However, the question regarding how to optimally configure the RMS through the transition phase, i.e., ramp-up and ramp-down, from one product family to another, is still an issue where production organizations and managers need greater decision support. The case study in this paper, see section 5, presents such a scenario taken from the automotive industry. The company is currently producing a single set of crankshafts, including some variants with the product family. In parallel to this, they are currently initiating a production ramp-up of a new product family of crankshafts, thus facing the above-stated issue of how optimally configure the production resources through this transition whilst still reaching the production target levels, such as throughput, buffer capacity, etc. Here, SMO is utilized to provide the decision support to the production managers on how to reconfigure their production resources whilst maximizing throughput and minimizing buffer capacities for each possible production configuration setup through the ramp-up and ramp-down of the two product families.

## IV. A SMO APPROACH

### A. THE OVERALL METHODOLOGY: HOW TO USE SMO FOR OPTIMIZING RMS RE-CONFIGURATIONS

Decision support using the SMO approach in manufacturing systems design and improvement projects can be represented by four iterative loops consisted of four main activities, as shown in Fig. 2. Loop (1) consists of the start phase when the problem is analyzed and formulated into a simulation-optimization problem. It is often overlooked that decision-making activities, here referring to not only the final decision for implementation but also any decisions involved during the whole project, which would affect the final outcomes of the analysis, results and the final decision. This is an important point to note because deciding what decision variables to be included, their ranges and other constraints as well as which simulation outputs are included in the SMO as the optimization objectives all directly affect the selection of the abstraction level and simulation modeling represented as Loop (2). These optimization settings, including objectives, decision variables and constraints, are the inputs to "*Multi-Objective Optimization*", see Loop (3). In return, the optimization activity sends back the results from the SMO-loop representing the outputs of the optimization, i.e., Loop 4, in terms of Pareto-optimal solutions to "*Decision Making*" for choosing the final solution (Loop (3)). It is also possible that the decision-maker can adjust the final solution, possibly to be verified with the simulation and compare with the results from the SMO run.

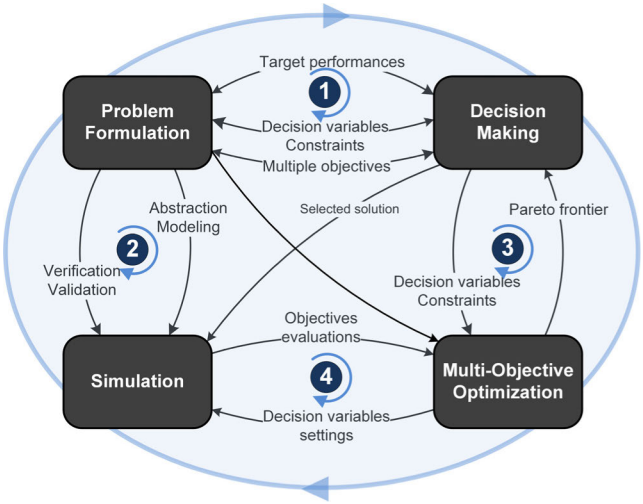


**FIGURE 2.** SMO loop.

In terms of MOO, to the best of our knowledge, the SMO approach in this specific study is the first that simultaneously maximizes THP and minimizes TBC while providing the optimal MPFL configuration and task allocation for fluctuating production volumes and scalable capacities. In other words, this approach determines how to obtain the highest possible THP with the minimum number of buffers considering different numbers of machines and production volumes, including buffers and task allocation. This could support not only individual product volume changes but also the system scalability aspect (total production volumes), providing the optimal way to add resources (machines and buffers) or reconfigure existing ones to meet new demand scenarios.

The number of aspects simultaneously considered by this approach increases the complexity of the problem exponentially. The SMO consists of two main components, the simulation model and the optimization engine. The process starts with a feasible solution is generated in the simulation model. The simulation model enables the input parameters combination and experimentation following the optimization objectives and the system constraints to find the optimal output solutions. This is an iterative process in which the optimization engine processes the outputs of the simulation as the values of the objective functions in order to assign a new combination of input parameters so as to converge to a set of near-optimal values for the decision variables over time. The SMO approach and its mechanisms are graphically illustrated in Fig. 3. Optimization methods can be classified into exact and non-exact methods. Exact methods like mathematical programming or $\varepsilon$ constraints and non-exact like metaheuristics which include the trajectory and population-based methods, have been previously applied to similar problems. However, when considering the RMS challenges in a multi-objective optimization context, population-based metaheuristic methods have been identified as one of the most powerful optimization methods and Genetic Algorithm (GA) as the most efficient in nearing optimal solutions [12]. Therefore, this approach employs the well-known fast elitism non-dominated sorting genetic algorithm II (NSGA-II) [45] for optimization due to its efficiency in handling multi-objective problems with 2 or 3 objectives.

The optimization objectives in this study are defined in Equations (1) to (3). The considered constraints are presented in Equations (4) to (11).

**List of symbols**

| | |
|---|---|
| $j$ | *workstation index.* |
| $S$ | *number of workstations.* |
| $i, r$ | *tasks index.* |
| $N$ | *number of tasks.* |
| $k$ | *machines index.* |
| $M$ | *total number of machines in the RMS.* |
| $m_{max}$ | *maximum number of machines per workstation.* |
| $M_{min}$ | *minimum number of machines in the RMS that must be assigned for production.* |
| $B_{min}$ | *minimum safety buffer.* |
| $B_{max}$ | *maximum buffer capacity.* |
| $B_j$ | *buffer capacity for workstation j.* |
| $P$ | *Set of precedence relationships $(r, i \in P$ if and only if task $r$ is an immediate predecessor of task $i$).* |
| $x_{ij}$ | *1 if task i is assigned to workstation j; 0 otherwise.* |
| $y_{kj}$ | *1 if machine k is assigned to workstation j; 0 otherwise.* |

Three conflicting optimization objectives are defined as follows.

$$Maximize\, f1 = THP : Throughput\ (jobs\ per\ hour) \tag{1}$$

$$Minimize\, f2 = \sum_{j=2}^{S} B_{j-1} : Total\ Buffer\ Capacity \tag{2}$$

$$Minimize\, f3 = \sum_{k=1}^{K_{max}} \sum_{j=1}^{J} y_{kj} : Number\ of\ Machines \tag{3}$$

The following constraints have to be fulfilled when optimizing the RMS.

Task allocation: each task can only be assigned to one workstation:

$$\sum_{j=1}^{S} x_{ij} = 1, \quad \forall i = 1, 2, \ldots, N \tag{4}$$

Precedence relation: a task is assigned to a station only if all its predecessors are assigned to the same or earlier workstations:

$$\sum_{j=1}^{S} j\left(x_{rj} - x_{ij}\right) \leq 0, \quad \forall (r, i) \in P \tag{5}$$

Machine allocation: each machine must only be assigned to one workstation:

$$\sum_{j=1}^{S} y_{kj} = 1, \quad \forall k = 1, 2, \ldots, M \tag{6}$$

Technological requirement - a task is allocated to a workstation if it has the required machinery to execute the task:

$$C_{ik} \times x_{ij} \leq y_{kj} \quad \forall k = 1, 2, \ldots, M; i = 1, 2, \ldots, N; \; j = 1, 2, \ldots, S \tag{7}$$

Workstation utilization: at least one machine should be assigned to each workstation:

$$\sum_{k=1}^{M} y_{ki} \geq 1, \quad \forall j = 1, 2, \ldots, S \tag{8}$$

Floorspace limitation - each workstation cannot have more than a certain number of machines:

$$\sum_{k=1}^{M} y_{kj} \leq m_{\max}, \quad \forall j = 1, 2, \ldots, S \tag{9}$$

Machine utilization- the assigned machines to workstations cannot exceed the total number of available machines. Moreover, to ensure production, a minimum number of machines should be assigned to workstations:

$$M_{min} \leq \sum_{k=1}^{K_{max}} \sum_{j=1}^{J} y_{kj} \leq M \tag{10}$$

Buffer capacity limitations- each inter- stations buffer should not become less than a certain safety capacity and should not exceed a maximum buffer size:

$$B_{min} \leq B_{j-1} \leq B_{max} \quad j = 2, \ldots, S \tag{11}$$

The applicability of this approach is demonstrated by an illustrative example in Section 4.3 and then an industrial-inspired case described in Section V.

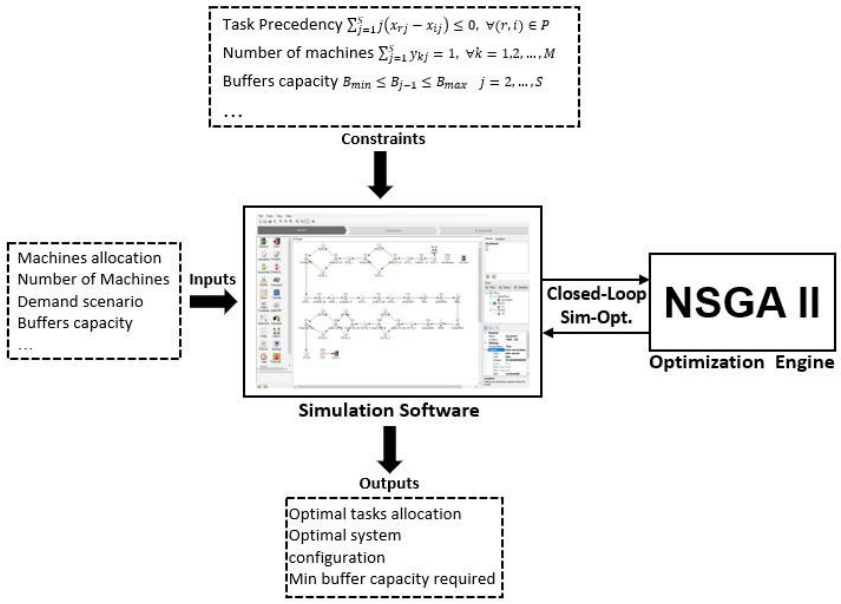


**FIGURE 3.** Graphical representation of the SMO.

### B. OPTIMIZATION ALGORITHM DETAILS

Genetic algorithms have been extensively used to optimize production and manufacturing systems [46]. NSGA-II is one of the most used multi-objective evolutionary algorithms (MOEA) [13]. The designed combination of the fast non-dominated sorting approach and the crowding distance calculation to sort and rank the solutions stated by their fitness value endow the well-balanced convergence and spread required by any efficient MOEA [41]. When compared to its earlier version, the elitist mechanism of the NSGA-II combines the best parents with the best offspring obtained from the genetic operations, see Fig. 5.

#### 1) FAST NON-DOMINATED SORTING

There are three major techniques that render the outstanding performance of NSGA-II [47]: (1) a fast non-dominated sorting approach that reduces the computational complexity in other GA-based MOEA; (2) the elitism selection procedure described above; and (3) the use of crowding distance, as a measure for comparison and selection after the non-dominated sorting, to preserve the diversity of the solutions in the population. Fast non-dominated sorting is the procedure to efficiently sort the solutions into multiple fronts with different ranks based on their dominance relationships. For each couple of solutions (S1, S2), three types of relationships can be established: solution S1 dominates solution S2, solution S1 is dominated by solutions S2, and lastly, neither of them dominates each other (i.e., they are non-dominated). This dominance relationship is established by comparing the objectives set by the values (fitnesses) of the objective functions. When the comparison of all different solutions in the population is made, the non-dominated solutions will form the first front (rank 1) of solutions in the current population. Then the same process will be repeated in the same population, excluding the first front from the population to find the second-best front (rank 2) of solutions. This process is repeated iteratively until all solutions are classified into different fronts, as shown in Fig. 4.

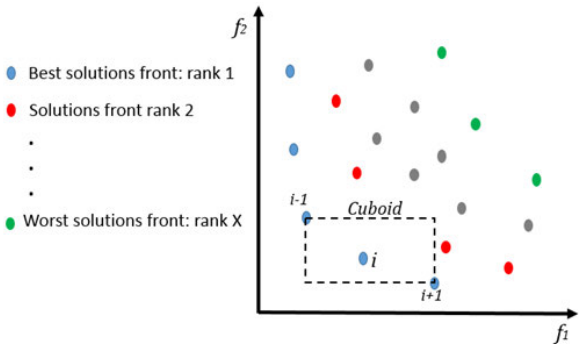


**FIGURE 4.** Fast non-dominated sorting and crowding distance calculation.

#### 2) CROWDING DISTANCE

To ensure a good spread of solutions, it is important to determine the density of the solutions when selecting the solutions to be preserved into the next generation. The crowding distance calculation procedure helps to determine the rank of the solutions in the same front once the fast non-dominated sorting is completed. This is attained by assigning to every solution the average side distance of the cuboid (shown as a dashed box) formed by the nearest solution points on the same front with the same rank, see Fig. 4. Consequently, the crowding distance calculation helps to determine the most dispersed (i.e., less crowded) solutions of the front. These solutions will have a preference to be preserved for the next generation to ensure a more diverse population.

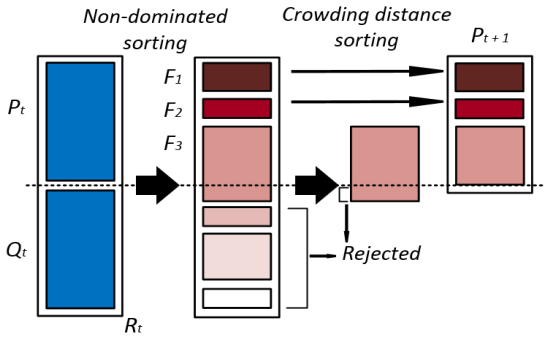


**FIGURE 5.** NSGA II implementation. Inspired by [41].

### 3) CROSSOVER AND MUTATION OPERATORS OF NSGA II

For the generation of the new population, NSGA II uses the crossover and mutation operators. The crossover operator takes place between two solutions. This operator randomly intersects the chromosome of two solutions and then combines the genes from different parts of the chromosome of each solution to generate two new solutions. As inspired by the biological mutation, this operator occurs randomly in each generation to maintain the diversity from one generation to the next. This operator modifies one or several genes/points in the solution/chromosome according to the mutation probability. As the mutation probability increases, the more changes the solution will occur. Therefore, with a high mutation probability, the solution may change completely from the previous one.

The implementation of the NSGA II, according to [45], is conceived as in Fig. 5. Applying the crossover and mutation operators to a population $P_t$, $Q_t$ offspring of size N is generated. Then a combined population is sorted applying the previously explained fast non-dominated sorting and crowding distance comparison. To create the N best solutions that become the next population $P_{t+1}$. $F_1$, $F_2$, and $F_3$ represent the best, second best, and third best non-dominated sets of solutions in the new combined population. The combined population is determined by $R_t$, the union of $P_t$, and the offspring $Q_t$, so $R_t = Q_t \cup P_t$. Finally, the solutions from the set $F_1$ have the highest priority to remain, the solution in $F_2$ the second-highest priority, and so on. As a summary, the major steps followed by the NSGA II algorithm are illustrated by the flowchart in Fig. 6.

### 4) GENETIC REPRESENTATION AND CONSTRAINT HANDLING

In this study, the chromosome of the problem is represented by a gene vector of integer numbers which is initially randomly generated from concatenating different encoded real-valued genes into one chromosome. Such a vector consists of three sub-strings of genes. The first sub-string represents the number of machines assigned to the reconfigurable WSs. The second sub-string represents machining task assignment to WSs regardless of the number of parts considered in the problem and the third one represents the

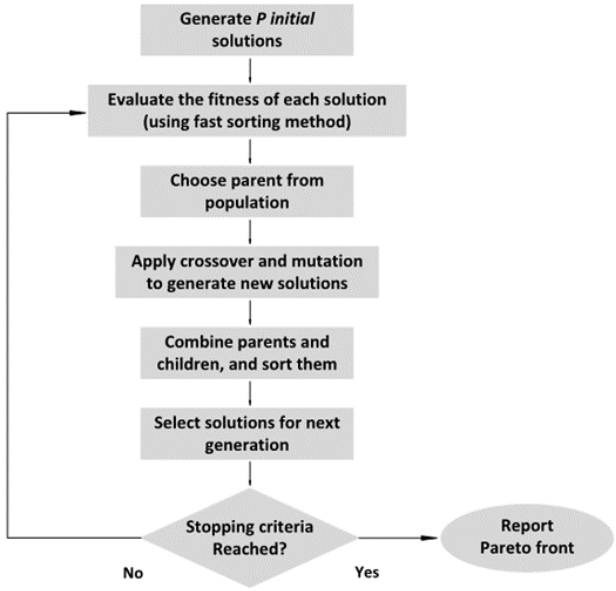


**FIGURE 6.** NSGA II flowchart. Inspired by [41].

buffer capacities allocation. The length of the vector L is equal to the sum of the lengths of these three sub-strings.

The first sub-string of the gene vector that represents the number of machines per WS has a length determined by the number of WSs that can add or remove machines to cope with production changes. Then, each position in this part of the vector represents a specific WS and receives an integer with a value between 1 and $m_{max}$ (i.e., the maximum number of machines per workstation), which represents the number of machines assigned to that specific WS. The total number of machines used in all WSs is bounded by Constraint (9).

The next sub-string of the vector, task assignment, represents whether the tasks are performed on the specific WSs and its length is the number of reconfigurable WSs times the number of manufacturing tasks to be assigned to the WSs. As an example, if there are five tasks of part A and six tasks of part B to be distributed in 2 WSs, the length of this segment of the vector becomes 22. This segment only receives binary numbers: 1 if a task is performed in the considered WS and 0 if it is not. It is important to note that each task can only be performed by a workstation and the precedence of the tasks are ensured by Constraints (3) and (4) together.

The last gene of the vector represents the capacity of every buffer in the manufacturing line and its length is equal to the number of buffers in the line. In this part, integer values are generated in a range between $B_{min}$ and $B_{max}$, minimum safety buffer and maximum buffer capacity as formulated in Constraint (10).

Fig. 7 shows the solution representation for a simplified example with two WSs, two tasks to be assigned, and one inter-station buffer to allocate its capacity. In this example, there are 3 machines in the first WS, 2 machines in the second WS, task 1 is performed in the first WS, task 2 in the second WS, and the buffer has a capacity of 200.

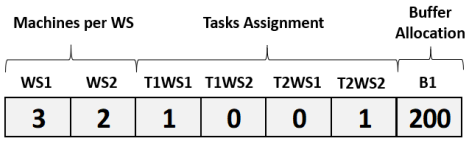


**FIGURE 7.** Solution representation simplified example.

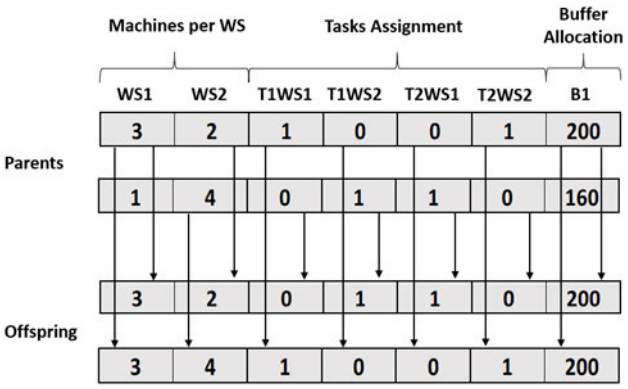


**FIGURE 8.** Crossover operator.

In the case of this study, the genetic operators, crossover and mutation, works independently in the three different parts of the vector.

A uniform crossover operator is used to generate two offspring from two parent solutions [48]. In this type of crossover, every bit of the string in the offspring takes a value from either of the parents. In this case, after the parents are randomly selected, the bits of the offspring have the same probability of taking a value from the same bit of either of the parents. Fig. 8 illustrates the process of this crossover where the arrows indicate from which parent the bits of the offspring have copied their values.

A uniform mutation operator was employed to maintain diversity in future generations. This type of mutation randomly selects one or several bits from the parent, which will be mutated in the offspring. The non-mutated bits in the offspring are maintained from the parent. The higher the mutation probability, the more bits will be mutated in the offspring. In the case of this study, the mutated bits have an equal probability of taking any possible value according to the defined constraints. Fig. 9 illustrates the uniform mutation operator, where the dark positions in the offspring represent the mutated bits from the parent. Considering that genetic operators work independently in the different parts of the vector, in the illustrated example of Fig. 9, the offspring has one mutated bit in the machines per WS string, two mutated bits in the task assignment string, and one mutated bit in the buffer allocation string.

A repairing procedure is activated when no feasible solution has been reached with the genetic operators. In the studied problem, the constraints ensure, among other aspects, the limited number of machines per WS, the total number of machines in the system, technological constraints, the precedency of the tasks, and that buffers take a feasible capacity. Therefore, this becomes a highly constrained combinatorial

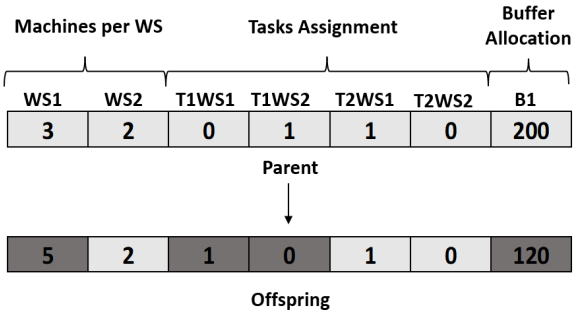


**FIGURE 9.** Mutation operator.

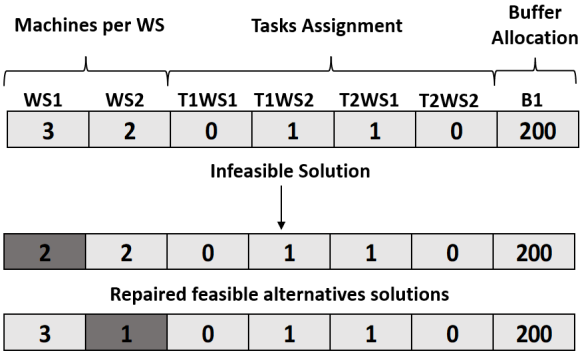


**FIGURE 10.** Solution repair method example.

optimization problem that creates many unfeasible solutions that need to be repaired.

The repairing method used consists of finding the nearest feasible solution. This is achieved by solving a mixed-integer programming (MIP) problem that aims at minimizing the distance between the unfeasible solution and the closest feasible solution. When the minimum distance from an infeasible solution to a feasible solution can be obtained with several feasible solutions, then one of these feasible solutions is randomly selected. If we consider the total number of machines in the system to be constrained to be equal to 4, Fig. 10 represents the example of how an infeasible solution would be repaired. In the shown example, two feasible alternatives solutions have the same probability to be selected.

### C. AN ILLUSTRATIVE EXAMPLE

This sub-section presents the SMO results from a hypothetical RMS model to illustrate the applicability of the proposed approach. In this illustrative example, all of the three optimization objectives presented in equations (1)-(3) were applied. This model consists of a machining process that takes 960 seconds, divided into 36 tasks. Due to space limitations and the technological constraints of the machining processes, some tasks (i.e., 3, 17, and 33) need to be performed in three different types of machines. The process is subject to realistic disturbances wherein machine availability is considered to be 90%, with a mean time to repair (MTTR) of 5 minutes. The RMS consists of three workstations with two inter-station buffers. Machines in the same workstation perform the same task sequence. There is space for up to 6 machines in each

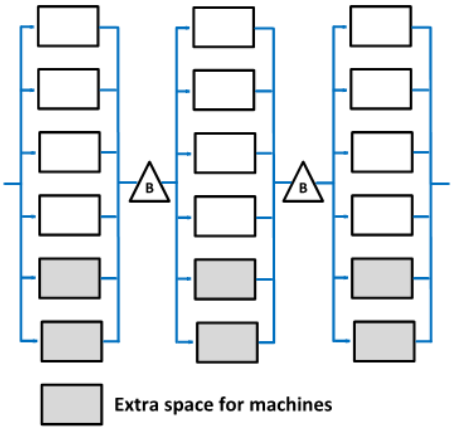


**FIGURE 11.** A simplified example.

**TABLE 1.** Throughput and buffers capacity.

| Number of machines | THP | B1 | B2 | TBC |
|---|---|---|---|---|
| 12 | 40.226-41.261 | 5-30 | 5-30 | 10-60 |
| 13 | 43.423-44.045 | 5-20 | 5-25 | 10-45 |
| 14 | 46.781-47.708 | 5-25 | 5-25 | 10-45 |
| 15 | 50.17-50.56 | 5-10 | 5-25 | 10-30 |
| 16 | 52.77-53.916 | 5-35 | 5-45 | 10-80 |
| 17 | 56.136-56.996 | 5-50 | 5-50 | 10-85 |
| 18 | 58.288-59.135 | 5-30 | 5-25 | 10-55 |

workstation. A minimum of 12 machines (i.e., $M_{min} = 12$) can be used in the system. Within the context of RMS, it is assumed that these installed machines can be moved around the workstations or removed and then added back later in future configurations, dependent on whether scaling down or up of the system is needed Fig. 11 shows a system started with four machines in each workstation and possesses extra space for up to two extra machines in each workstation (i.e., $m_{max} = 6$). Therefore, the RMS taken into account can vary from 12 to 18 machines distributed in three workstations, hence, $M_{max} = 18$.

The non-dominated solutions generated from SMO for this simplified model are presented in TABLE 1. It lists the solution ranges for the THP when $M$ increases from 12 to 18 and for the buffer capacities, $B_1$ and $B_2$, between the workstations needed for achieving that THP. TBC is the second objective in the optimization, which refers to the total buffer capacity capacities in the RMS ($B_1 + B_2$). An important insight elicited immediately by checking the results in TABLE 1 is that the optimized average THP increase that can be gained from every machine added to the system is approximately 2.97 JPH (Jobs Per Hour). This is important for the engineers to consider when scaling up (or down) of the system to adjust the production volume required.

TABLE 2 presents how the results for system configuration and task allocation presented in TABLE 1 can be achieved. WS1, WS2, and WS3 represent the number of parallel machines in workstations 1, 2, and 3, respectively. The fifth column shows the number of tasks performed in each workstation (i.e., no. of tasks assigned to workstation 1/no. of tasks to workstation 2/no. of tasks to workstation 3).

**TABLE 2.** Configuration and work tasks allocation.

| Number of machines | WS 1 | WS 2 | WS 3 | Tasks per Workstation |
|---|---|---|---|---|
| 12 | 2 | 4 | 6 | 5/14/17 |
| 13 | 2 | 6 | 5 | 4/19/13 |
| 14 | 2 | 6 | 6 | 4/17/15 |
| 15 | 3 | 6 | 6 | 6/16/14 |
| 16 | 6 | 5 | 5 | 16/10/10 |
| 17 | 6 | 5 | 6 | 15/9/12 |
| 18 | 6 | 6 | 6 | 13/12/11 |

Note that the number and location of the machines presented in Table 2 cannot be implemented in a rigid system wherein installed machines are not movable. Therefore, in order to scale up a rigid system, the reconfiguration steps need to consider the existing system architecture. Therefore, for such a system, every new configuration needs to reuse the previous layout to achieve the next level of configuration. Considering this constraint, Fig. 12 presents the reconfiguration steps if the system would be scaled up from 12 to 18 machines. Similarly, only the THP and TBC ranges of the non-dominated solutions are presented here. In addition, this figure also shows the number of tasks performed in each workstation for the different configurations obtained from the optimization in order to obtain the THP range presented.

Another directly visible result from Fig. 12 is how the consideration of a rigid system changed the configuration presented in TABLE 2 for the system with 12, 13, 14, and 15 machines. Therefore, instead of 2-4-6 for 12 machines, 2-6-5 for 13 machines, 2-6-6 for 14 machines, and 3-6-6 for 15 machines, they have been changed to 4-4-4, 5-4-4, 5-4-5, 6-4-5, respectively. Consequently, this represents a certain compromise in the THP for those configurations, as seen when comparing the configurations in Fig. 12 with TABLE 1.

Essentially, Fig. 12 provides a helpful understanding and view of the system, including the optimal location of additional machines if future capacity increases are needed. Knowing where to add machines in advance can be convenient and cost-effective when designing the system, especially when investing in the material handling system.

Another critical aspect of the design of manufacturing systems is the buffer capacity consideration. Fig. 12 also shows the optimized allocation of the buffer capacities for the given configurations. Essentially, Fig. 12 provides a helpful understanding and view of the system, including the optimal location of additional machines if future capacity increases are needed. Knowing where to add machines in advance can be convenient and cost-effective when designing the system, especially when investing in the material handling system.

TABLE 3 presents the total task time in seconds per workstation for the seven configurations in Fig. 12.

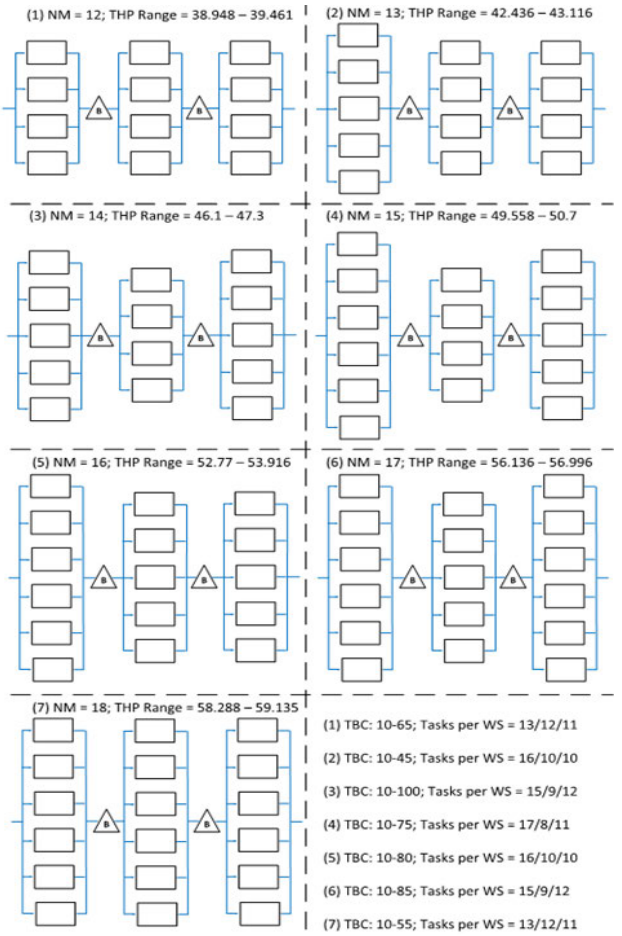


**FIGURE 12.** Reconfiguration steps, throughput (THP), total buffer capacity (TBC), and work task allocation.

**TABLE 3.** Total task time in seconds per workstation per configuration.

| Configuration Steps | Total Task Time per Workstation |
|---|---|
| (1) | 336/304/320 |
| (2) | 387/275/298 |
| (3) | 372/247/341 |
| (4) | 414/226/320 |
| (5) | 387/275/298 |
| (6) | 372/247/341 |
| (7) | 336/304/320 |

However, there are many more factors that can affect the decision-making tasks in manufacturing companies. The use of tools like the parallel coordinate plot (PCP) in Fig. 13 can support the knowledge elicitation and display which choices are available according to different constraints. Decision-makers can use this plot as a decision support tool and filter the solutions according to different constraints. In this PCP shown in Fig. 13, the columns from left to right represent the THP, the total number of machines ($M$), the number of machines in every workstation and the two buffer capacities (i.e., $B_1$ and $B_2$). In the current plot, solutions including 15, 16, and 17 machines have been colored in blue, red, and green, respectively, to show the considerable overlapping production rate and buffer capacity among the different numbers of machines. Accordingly, the PCP can help decision-makers visualize the optimized trade-offs between THP, the number of machines and buffer capacity to facilitate well-informed decision-making.

A concrete illustration of how decision-making can be supported is visualized in the throughput progression as the total buffer capacity, TBC, increases between 0 and 35 for the systems, presented in Fig. 14.

Fig. 14 shows that for this simplified manufacturing system, the curves indicate THP levels saturate early on, with respect to increasing TBC. On the other hand, different machine availability and MTTR values could significantly impact this relationship. Nonetheless, the red parallel dashed lines revealed that M number of machines, for some TBC values, can provide the same THP as M + 1 machines. Hence, the PCP can support decision-makers with the visualization and understanding of this trade-off situation in which the capacity of the system can be increased, either by adding machines or buffer capacity.

## V. AN INDUSTRIAL APPLICATION

This section presents an industrial application study in an automotive manufacturer to illustrate the proposed SMO approach. The case is based on a 4-cylinder crankshaft production line. A crankshaft is a key component of an engine. It includes, in addition to several bearing surfaces, channels for lubrication and a threaded stem for driving such generators and other external components in an engine. The number of bearing surfaces is influenced by the size of the crankshaft, which is controlled by the number of cylinders in the engine and its configuration.

The production line manufactures two product families. It consists of 18 WSs wherein processes including unpacking, milling, mass balancing, turning, drilling, deburring, grinding, washing and quality control are performed together with 17 inter-station buffers. The company invested in reconfigurable/modular CNC machines which are placed in the bottleneck and most critical part of the line, WSs 90, 100 and 110. Unlike the rest of the machines used in the line, the modular machines can be added to the reconfigurable WSs and moved to be employed in other reconfigurable WSs if needed due to production changes. The simulation model is shown in Fig. 15 in which the dashed area represents where the reconfigurable WSs of the line are placed. Moreover, this MPFL is subjected to uncertainty and variability - all machines in the system consider a specific availability and MTTR and setup time when switching product types. When it comes to the three reconfigurable WSs, machine availability is considered 87.41% of processing time with MTTR = 3 hours and 1 min setup time when switching between different part types. Each buffer has a minimum safety buffer $B_{min} = 20$ and a maximum buffer capacity $B_{max}$. The buffers employed use a rack system to adjust the capacity. Each buffer fits up to 15 racks and each rack can fit

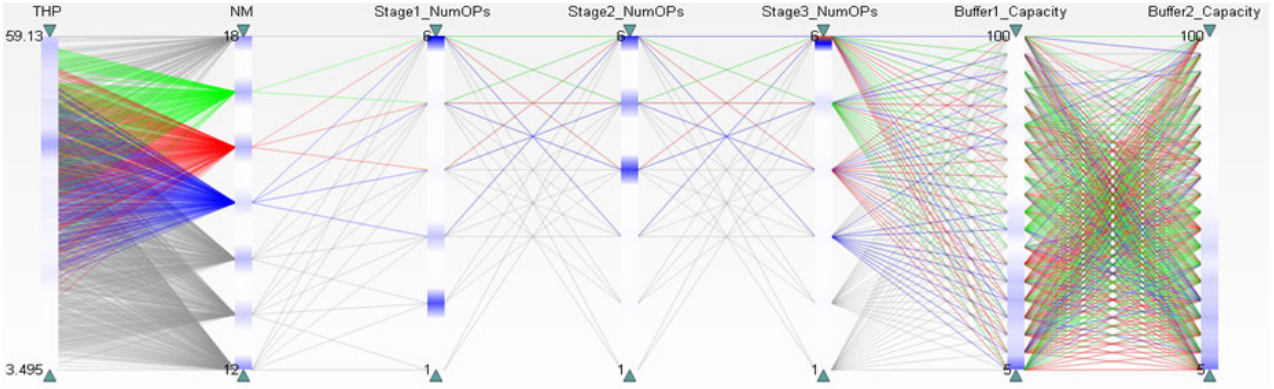


**FIGURE 13.** Parallel coordinate plot relating THP with the decision variable.

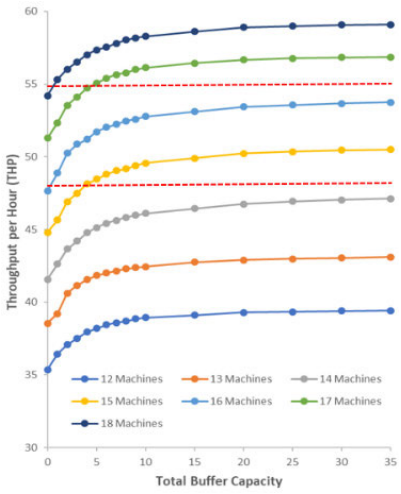


**FIGURE 14.** Optimized total buffer capacity vs. throughput mapping.

up to 20 parts. Therefore, $B_{max}$ becomes 300. In addition, all buffers consume 5 seconds as the material handling time that should not be neglected in the simulation model.

Unlike the previous example presented in Section 4.3, the reconfigurable WSs in this industrial case can add, remove and relocate machines according to the production needs. In each of these three WSs, there is space for up to 5 modules (machines). Fig. 16 represents an example of the three reconfigurable WSs when they have 7 machines, configured in a 4-1-2 setting, meaning 4 machines in WS90, 1 in WS100 and 2 in WS110. In this example, it remains space for 1, 4, and 3 extra machines in WS90, WS100, and WS110, respectively.

In this study, both parts in the considered MPFL need to be produced at a certain volume to meet the customers' demands. As such demands fluctuate and change over time, the configuration of the WSs 90, 100, and 110 evolve accordingly to meet the demand changes. The changes in the WSs affect not only the layout and the total number of machines needed in the aforementioned reconfigurable WSs, but also the tasks assigned to them. Also, as the demand changes, the reconfigurable configuration evolves, impacting the capacity of the buffers needed for the line. Our company has to investigate how much they could produce with an initial investment of 7 reconfigurable machines in the aforementioned WSs for different proportions of part 1 and part 2, 80/20 (80 % part 1 and 20 % part 2), 60/40, 40/60, and 20/80. Furthermore, it is also useful to know the production capacity that can be gained from every machine added to the system, including where to add it, according to the desired production proportions and how the re-allocation of the machining tasks of part 1 and part 2 can be optimized. This study aims at attaining the maximum THP with the minimum TBC; apart from the optimized TBC, the results have to tell the capacity of every buffer in the line according to all the scenarios studied.

The sequence and times of the machining tasks of the produced parts are considerably different. The total machining times of the two parts for the reconfigurable WSs (90, 100, and 110) are 256 seconds divided into 15 tasks for part 1 (4cylP), and 274 seconds divided into 10 tasks for part 2 (4cylD). The task precedence for both parts is shown in Fig. 17. The machining processes of these three WSs involve milling, drilling of oil holes, and turning main bearings and tap. Due to technological constraints, tasks 1, 2, and 11 for part 1, and 1, 9, and 10 for part 2 need to be performed in different WSs.

## VI. RESULTS AND ANALYSIS

This section presents the results of the optimization for the previously explained scenarios, modifying the production proportions from 80% of part 1 and 20 % of part 2 to the opposite scenario 20% of part 1 and 80% of part 2, considering 20% steps changes in between the scenarios. Moreover, each of the mentioned proportions was investigated with 7, 8, and 9 machines in the reconfigurable WSs. Consequently, there are in total 12 scenarios to optimize.

Every scenario was optimized individually using NSGA II with 15000 iterations. An SMO software called FACTS Analyzer [49], in which a DES engine and various optimization algorithms are tightly integrated, was used for modeling the studied manufacturing line and carrying out all the optimization runs. This software allows to include almost all model variables (e.g., processing times, times to repair

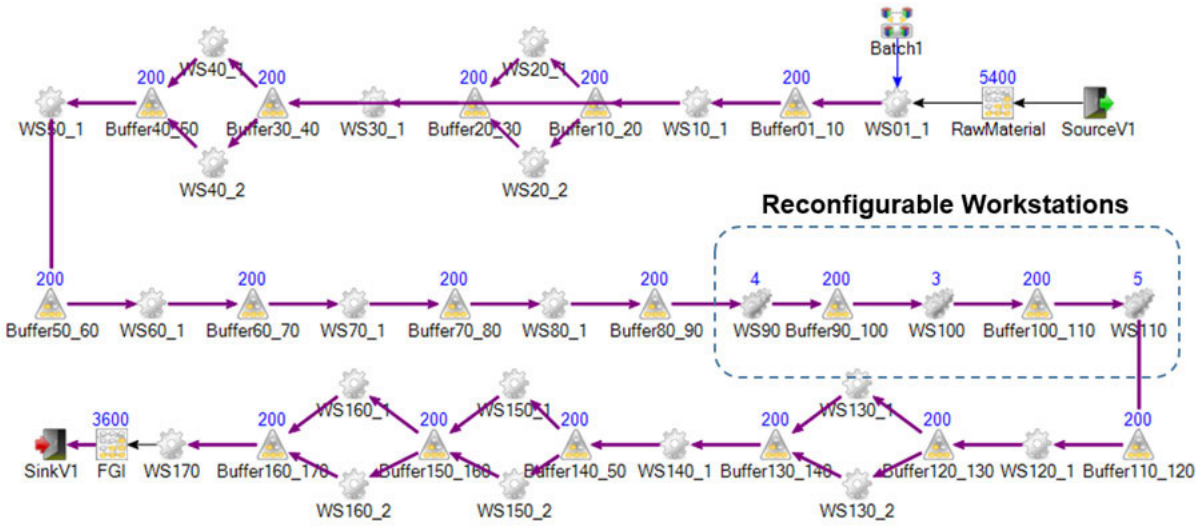


**FIGURE 15.** Simulation model representation of the production line.

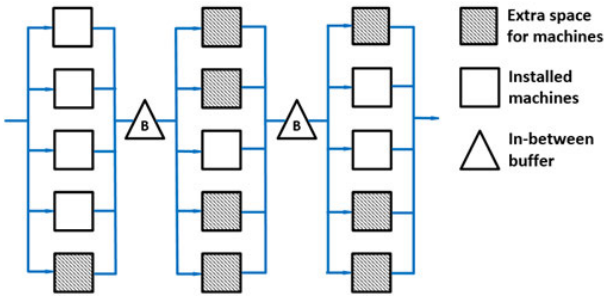


**FIGURE 16.** Reconfigurable workstations layout.

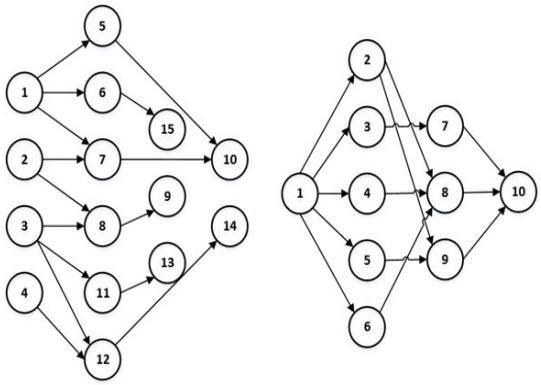


**FIGURE 17.** Precedency graphs.

and buffer capacity), regardless of their nature (continuous variables or integers), as decision variables and constraints for the optimizations. In this way, the simulation model serves for the iterative implementation for all possible combinations of the input variables according to the objectives defined by equations (1) and (2), and the constraints of the optimization defined in section 4.

Fig. 18 illustrates the optimized configurations and the required changes to cope with the studied scenarios in the reconfigurable WSs of the line. Each quadrant in the figure represents a production proportion. The white machines describe the machines included a 7-machine configuration, the light and dark grey machines describe where to add a machine for an 8 and 9 machines configuration, respectively. Then, for the 7-machine scenarios, only white machines need to be considered; for the 8-machine scenarios, white and light grey need to be considered, and for the 9-machine scenarios, all represented machines need to be considered. NM represents the number of machines, so in each quadrant of the figure is shown, the configuration and the THP range obtained for every number of machines considered for the different production proportions.

Considering the maximum THP in each of the studied scenarios, as seen in Fig. 18, the average THP gained per machine added regardless of the production proportions is 7.36. However, the results show an overlapping in THP as the number of machines increases. For a better understanding of this THP overlapping, Fig. 20 displays on the upper part the THP ranges (minimum and maximum THP included in the Pareto front depending on the TBC) for every scenario. Furthermore, the lower part of the figure illustrates the THP evolution as the TBC increases from 340 to 1100 for 7, 8 and 9 machines when the volume proportions are considered to be 80% part 1 and 20% part 2. The figure displays how different number machines in the reconfigure WSs can share the same THP range. Every solution from the optimization presents the required information for the production of a particular volume in different proportions. This information includes, for a determined THP, the required TBC and how they are allocated among the buffers in the line, the assignment of machines to the reconfigurable WSs, and tasks assigned to them. When focusing on the conflicting optimization objectives THP and TBC, the parallel coordinate plot can support the interpretation of their relationship.

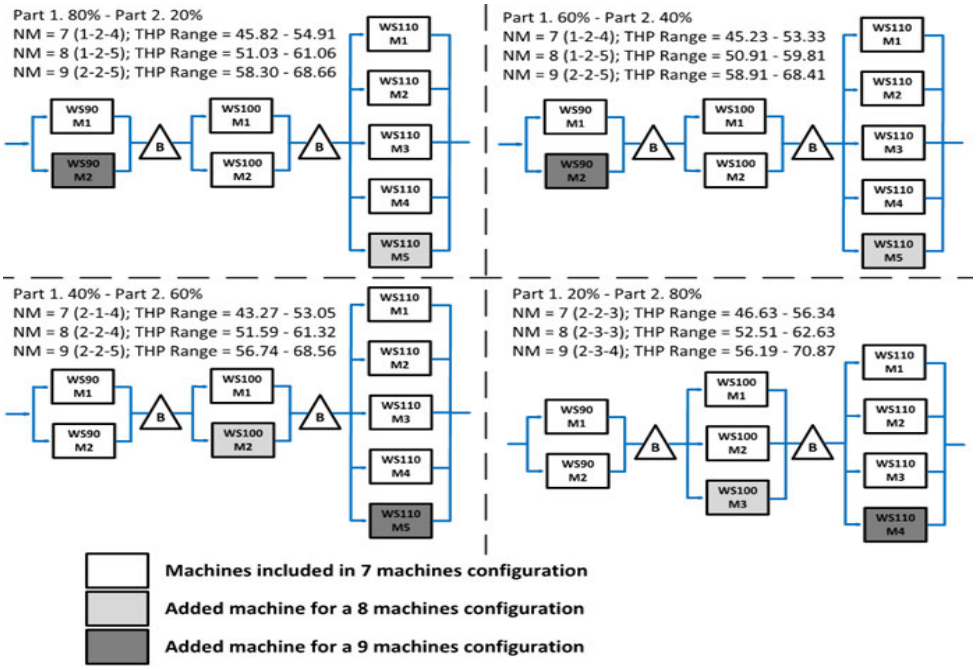


**FIGURE 18.** Optimized configurations for the studied scenarios.

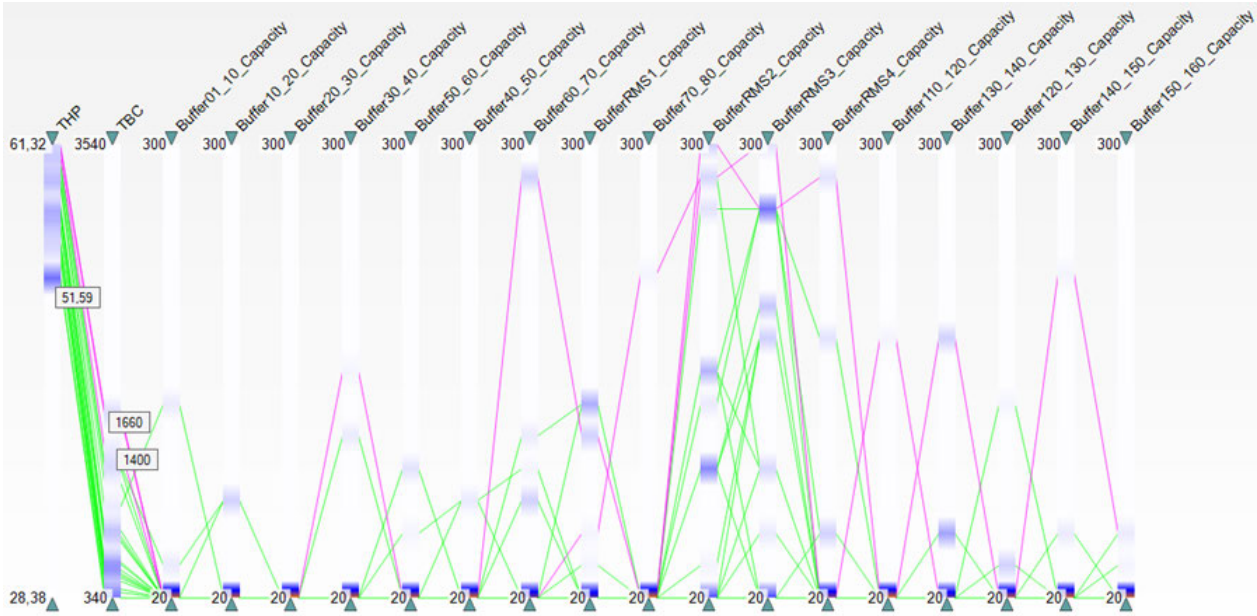


**FIGURE 19.** Parallel coordinate plot over THP, TBC, and buffers.

As an example, Fig. 19 displays, in the parallel coordinate plot, the non-dominated solution for the scenario where the reconfigurable WSs employ 8 machines and the line is producing in a proportion of 40% of part 1 and 60% of part 2. The columns represent the THP, TBC, and all individual buffers of the system. In this scenario, the lowest THP included in the Pareto front is 51.59 and is reached with a TBC of 340, and the highest THP is 61.32 reached with a TBC of 1660. This plot, besides revealing the trade-off between the objectives, also includes details about every individual buffer in the system. As an example of how this plot could support decision-makers, specific filters or rules could be set to simplify the understanding. In this case, the non-dominated solutions which a THP higher than 60 are represented with the purple lines and lower than 60 with the green line. As indicated in the figure, the solutions with THP higher than 60 have a TBC range between 1400 and 1660. Moreover, every solution includes information on the specific capacity of each buffer in the system. Therefore, rules can be used to reveal and simplify the understanding of how variables

**TABLE 4.** Task assignment for maximum THP.

| | Number of Machines 7 | | | | Number of Machines 8 | | | | Number of Machines 9 | | | |
|---|---|---|---|---|---|---|---|---|---|---|---|---|
| | 80/20 | 60/40 | 40/60 | 20/80 | 80/20 | 60/40 | 40/60 | 20/80 | 80/20 | 60/40 | 40/60 | 20/80 |
| *Tasks* | 1-2-4 | 1-2-4 | 2-1-4 | 2-2-3 | 1-2-5 | 1-2-5 | 2-2-4 | 2-3-3 | 2-2-5 | 2-2-5 | 2-2-5 | 2-3-4 |
| *Part1* | | | | | | | | | | | | |
| *1* | WS90 | WS90 | WS90 | WS90 | WS90 | WS90 | WS90 | WS90 | WS90 | WS90 | WS90 | WS90 |
| *2* | WS100 | WS100 | WS100 | WS100 | WS100 | WS100 | WS100 | WS100 | WS100 | WS100 | WS100 | WS100 |
| *3* | WS90 | WS100 | WS90 | WS90 | WS90 | WS100 | WS90 | WS90 | WS90 | WS90 | WS90 | WS90 |
| *4* | WS90 | WS100 | WS90 | WS90 | WS90 | WS90 | WS90 | WS90 | WS90 | WS90 | WS90 | WS90 |
| *5* | WS100 | WS90 | WS90 | WS90 | WS100 | WS90 | WS90 | WS90 | WS90 | WS90 | WS100 | WS100 |
| *6* | WS100 | WS90 | WS90 | WS90 | WS100 | WS90 | WS90 | WS90 | WS90 | WS100 | WS90 | WS90 |
| *7* | WS110 | WS110 | WS110 | WS110 | WS110 | WS110 | WS110 | WS110 | WS110 | WS110 | WS110 | WS110 |
| *8* | WS100 | WS100 | WS100 | WS100 | WS100 | WS110 | WS100 | WS100 | WS100 | WS100 | WS100 | WS100 |
| *9* | WS100 | WS100 | WS100 | WS100 | WS100 | WS100 | WS100 | WS100 | WS100 | WS100 | WS100 | WS100 |
| *10* | WS110 | WS110 | WS110 | WS110 | WS110 | WS110 | WS110 | WS110 | WS110 | WS110 | WS110 | WS110 |
| *11* | WS110 | WS110 | WS110 | WS110 | WS110 | WS110 | WS110 | WS110 | WS110 | WS110 | WS110 | WS110 |
| *12* | WS100 | WS100 | WS90 | WS90 | WS100 | WS100 | WS90 | WS100 | WS100 | WS90 | WS100 | WS90 |
| *13* | WS110 | WS110 | WS110 | WS110 | WS110 | WS110 | WS110 | WS110 | WS110 | WS110 | WS110 | WS110 |
| *14* | WS110 | WS110 | WS110 | WS110 | WS110 | WS110 | WS110 | WS110 | WS110 | WS110 | WS110 | WS110 |
| *15* | WS100 | WS90 | WS90 | WS90 | WS100 | WS90 | WS100 | WS90 | WS90 | WS100 | WS90 | WS100 |
| *Part2* | | | | | | | | | | | | |
| *1* | WS90 | WS90 | WS90 | WS90 | WS90 | WS90 | WS90 | WS90 | WS90 | WS90 | WS90 | WS90 |
| *2* | WS100 | WS100 | WS90 | WS100 | WS100 | WS100 | WS90 | WS100 | WS100 | WS100 | WS90 | WS100 |
| *3* | WS100 | WS110 | WS110 | WS90 | WS110 | WS110 | WS110 | WS90 | WS110 | WS90 | WS110 | WS90 |
| *4* | WS110 | WS100 | WS100 | WS90 | WS90 | WS90 | WS100 | WS100 | WS90 | WS110 | WS90 | WS110 |
| *5* | WS90 | WS100 | WS90 | WS100 | WS100 | WS100 | WS90 | WS100 | WS90 | WS100 | WS100 | WS100 |
| *6* | WS110 | WS90 | WS90 | WS110 | WS110 | WS110 | WS100 | WS100 | WS90 | WS110 | WS100 | WS90 |
| *7* | WS100 | WS110 | WS110 | WS90 | WS110 | WS110 | WS110 | WS90 | WS110 | WS90 | WS110 | WS100 |
| *8* | WS110 | WS110 | WS110 | WS110 | WS110 | WS110 | WS100 | WS110 | WS100 | WS110 | WS110 | WS110 |
| *9* | WS100 | WS100 | WS100 | WS100 | WS100 | WS100 | WS100 | WS100 | WS100 | WS100 | WS100 | WS100 |
| *10* | WS110 | WS110 | WS110 | WS110 | WS110 | WS110 | WS110 | WS110 | WS110 | WS110 | WS110 | WS110 |

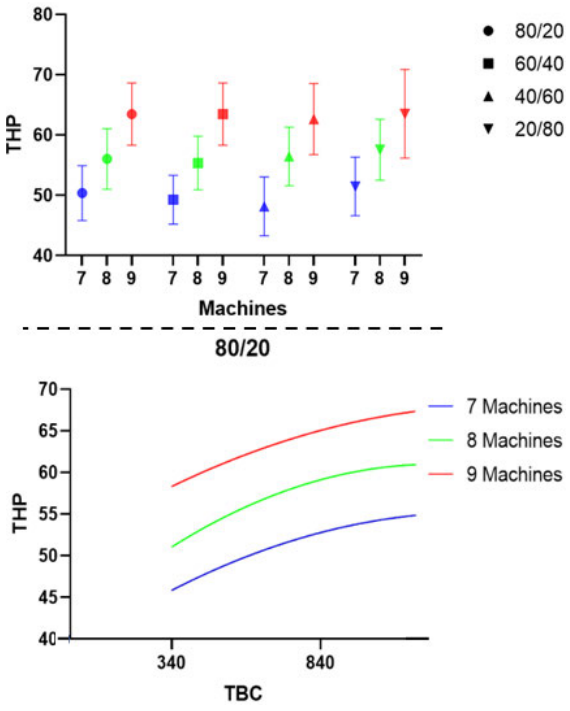


**FIGURE 20.** THP progression example.

affect the overall performance of the system. In the case represented in the figure, the purple lines can show which buffers are more important than others for getting THP over 60. Although all solutions included here are on the Pareto front, the highlighted solutions displayed in the PCP can give additional information about which buffers are more relevant for different decision-making scenarios and their capacities can be extracted and better understood with the graphical aid. This type of additional insight resulting from applying SMO enables a more confident decision-making process which is one of the advantages of this approach.

Another core tenant of this approach is the task assigned to WSs; TABLE 3 illustrates the task assignment to WSs for the maximum obtained THP in the studied scenarios. It presents the results from the optimization and provides details about how to rebalance the tasks and reconfigure the system as the production proportion and volume change. The three groups of columns in the table represent the system when there are 7, 8, or 9 machines in the reconfigurable WSs. The first three rows of the table, from top to bottom, indicate the total number of machines employed in the reconfigurable WSs, the volume proportion, and the number of machines per reconfigurable WS. In addition, the light, medium, and dark grey symbolize whether a task is performed in WS90, WS100, or WS110, respectively.

## VII. CONCLUSION AND OUTLOOK

RMSs are acknowledged to possess the capabilities that enable manufacturing companies to provide the required production capacity when needed. However, the research in real-scale industrial cases is still limited and often neglects the

variability of manufacturing systems so that inaccurate results can be produced. Furthermore, the use of SMO to deal with the RMS configuration problem and task assignments to WSs is sporadic. Against this backdrop and unlike other state-of-the-art methods, this article presented an SMO approach that simultaneously addresses the RMS configuration together with the tasks and resource assignment in an industrial-scalable MPFL for fluctuating production volumes. This approach also considers the unreliability of the equipment and deal with the buffer allocation dilemma - how many are needed and where to place them optimally. Consequently, it can be concluded that the proposed SMO approach provides support for the production planning and management of RMS when facing fluctuating production volumes. The applicability of the proposed SMO approach is not limited to manufacturing systems with modular machines and could also be applied to other types of RMS, such as human-based assembly/manufacturing systems, in which different configurations could be achieved through other means, e.g., employing a flexible material handling system like gantry robots. However, this would require adjustments in the approach to consider the new requirements.

Essentially, this study not only demonstrates the benefits that decision-makers could gain by adopting an SMO approach when selecting the RMS configuration and task assignment for fluctuating production volumes scenarios but also reveals a comprehensive amount of data that support the trade-off decisions inherent to a choice that requires rapid decision making and adaptation. To this extent, this study emphasizes the use of SBO in systems that may face fluctuating demands, which is one of the reasons for the adoption of an RMS beyond the design phase.

As discussed in the analysis of the results, rules can be used to reveal and simplify the understanding of how different RMS variables affect the overall performance of the system. A relatively recent research area within SMO is the extraction and utilization of knowledge from the optimization data using data mining because the Pareto-optimal solutions generated may reveal the clues about what constitutes the good solutions with respect to different criteria. Data mining methods can help to extract such patterns that may ultimately help the decision-maker in gaining a better understanding of solving the problem under different situations (e.g., demands). The knowledge gained can also be used in future related optimization scenarios. Such a process of generating and utilizing the knowledge within SMO is generally referred to as Knowledge-Driven Optimization [50]. Future research may also consider increasing the variety of the product families together with their volume proportion scenarios as studied in the current paper as well as including additional RMS aspects like reconfiguration frequency and the entire lifecycle of the system.

## ACKNOWLEDGMENT

The authors gratefully acknowledge their provision of research funding and thank one of the industrial partners in VF-KDO, Powertrain Engineering, Sweden, for their collaborative supports during this study.

## REFERENCES

[1] J. Dou, J. Li, D. Xia, and X. Zhao, "A multi-objective particle swarm optimisation for integrated configuration design and scheduling in reconfigurable manufacturing system," *Int. J. Prod. Res.*, vol. 59, no. 13, pp. 3975–3995, May 2020.

[2] Y. Koren, W. Wang, and X. Gu, "Value creation through design for scalability of reconfigurable manufacturing systems," *Int. J. Prod. Res.*, vol. 55, no. 5, pp. 1227–1242, Mar. 2017.

[3] Y. Koren and M. Shpitalni, "Design of reconfigurable manufacturing systems," *J. Manuf. Syst.*, vol. 29, no. 4, pp. 130–141, Oct. 2010.

[4] Y. Koren, U. Heisel, F. Jovane, T. Moriwaki, G. Pritschow, G. Ulsoy, and H. Van Brussel, "Reconfigurable manufacturing systems," *CIRP Ann.*, vol. 48, no. 2, pp. 527–540, 1999.

[5] Y. Koren, X. Gu, and W. Guo, "Reconfigurable manufacturing systems: Principles, design, and future trends," *Frontiers Mech. Eng.*, vol. 13, no. 2, pp. 121–136, 2018.

[6] M. Bortolini, F. G. Galizia, and C. Mora, "Reconfigurable manufacturing systems: Literature review and research trend," *J. Manuf. Syst.*, vol. 49, pp. 93–106, Oct. 2018.

[7] Y. Koren, X. Gu, and W. Guo, "Choosing the system configuration for high-volume manufacturing," *Int. J. Prod. Res.*, vol. 56, nos. 1–2, pp. 476–490, Jan. 2018.

[8] J. Dou, X. Dai, and Z. Meng, "Optimisation for multi-part flow-line configuration of reconfigurable manufacturing system using GA," *Int. J. Prod. Res.*, vol. 48, no. 14, pp. 4071–4100, Jul. 2010.

[9] K. K. Goyal, P. K. Jain, and M. Jain, "Optimal configuration selection for reconfigurable manufacturing system using NSGA II and TOPSIS," *Int. J. Prod. Res.*, vol. 50, no. 15, pp. 4175–4191, Aug. 2012.

[10] A. M. A. Youssef and H. A. ElMaraghy, "Modelling and optimization of multiple-aspect RMS configurations," *Int. J. Prod. Res.*, vol. 44, no. 22, pp. 4929–4958, Nov. 2006.

[11] A.-L. Andersen, T. D. Brunoe, K. Nielsen, and C. Rösiö, "Towards a generic design method for reconfigurable manufacturing systems: Analysis and synthesis of current design methods and evaluation of supportive tools," *J. Manuf. Syst.*, vol. 42, pp. 179–195, Jan. 2017.

[12] C. Renzi, F. Leali, M. Cavazzuti, and A. O. Andrisano, "A review on artificial intelligence applications to the optimal design of dedicated and reconfigurable manufacturing systems," *Int. J. Adv. Manuf. Technol.*, vol. 72, nos. 1–4, pp. 403–418, Apr. 2014.

[13] G. Michalos, S. Makris, and D. Mourtzis, "An intelligent search algorithm-based method to derive assembly line design alternatives," *Int. J. Comput. Integr. Manuf.*, vol. 25, no. 3, pp. 211–229, Mar. 2012.

[14] X. Delorme, S. Malyutin, and A. Dolgui, "A multi-objective approach for design of reconfigurable transfer lines," *IFAC-PapersOnLine*, vol. 49, no. 12, pp. 509–514, 2016.

[15] C. A. B. Diaz, T. Aslam, A. H. C. Ng, E. Flores-Garcia, and M. Wiktorsson, "Simulation-based multi-objective optimization for reconfigurable manufacturing system configurations analysis," in *Proc. Winter Simulation Conf. (WSC)*, Dec. 2020, pp. 1527–1538.

[16] D. Mourtzis, "Simulation in the design and operation of manufacturing systems: State of the art and new trends," *Int. J. Prod. Res.*, vol. 58, no. 7, pp. 1927–1949, Apr. 2020.

[17] S. E. H. Petroodi, A. B. D. Eynaud, N. Klement, and R. Tavakkoli-Moghaddam, "Simulation-based optimization approach with scenario-based product sequence in a reconfigurable manufacturing system (RMS): A case study," *IFAC-PapersOnLine*, vol. 52, no. 13, pp. 2638–2643, 2019.

[18] A. Bensmaine, M. Dahane, and L. Benyoucef, "A simulation-based genetic algorithm approach for process plans selection in uncertain reconfigurable environment," *IFAC Proc. Volumes*, vol. 46, no. 9, pp. 1961–1966, 2013.

[19] Y. Koren, S. J. Hu, and T. W. Weber, "Impact of manufacturing system configuration on performance," *CIRP Ann.*, vol. 47, no. 1, pp. 369–372, 1998.

[20] H. A. ElMaraghy, "Reconfigurable process plans for responsive manufacturing systems," in *Digital Enterprise Technology*, 1st ed., P. F. Cunha and P. G. Maropoulos, Eds. Springer, 2007, pp. 35–44, doi: 10.1007/978-0-387-49864-5_4.

[21] A. Azab, G. Perusi, H. A. ElMaraghy, and J. Urbanic, "Semi-generative macro-process planning for reconfigurable manufacturing," in *Digital Enterprise Technology*, 1st ed., P. F. Cunha and P. G. Maropoulos, Eds. Springer, 2007, pp. 251–258, doi: 10.1007/978-0-387-49864-5_29.

[22] W. Wang and Y. Koren, "Scalability planning for reconfigurable manufacturing systems," *J. Manuf. Syst.*, vol. 31, no. 2, pp. 83–91, Apr. 2012.
[23] A. M. A. Youssef and H. A. ElMaraghy, "Optimal configuration selection for reconfigurable manufacturing systems," *Int. J. Flexible Manuf. Syst.*, vol. 19, no. 2, pp. 67–106, Jun. 2007.
[24] P. Spicer and H. Carlo, "Integrating reconfiguration cost into the design of multi-period scalable reconfigurable manufacturing systems," *J. Manuf. Sci. Eng.*, vol. 129, no. 1, pp. 202–210, Feb. 2007, doi: 10.1115/1.2383196.
[25] J. P. Dou, X. Dai, and Z. Meng, "Precedence graph-oriented approach to optimise single-product flow-line configurations of reconfigurable manufacturing system," *Int. J. Comput. Integr. Manuf.*, vol. 22, no. 10, pp. 923–940, Oct. 2009.
[26] J. Dou, X. Dai, and Z. Meng, "A GA-based approach for optimizing single-part flow-line configurations of RMS," *J. Intell. Manuf.*, vol. 22, no. 2, pp. 301–317, Apr. 2011.
[27] S. K. Moghaddam, M. Houshmand, and O. Fatahi Valilai, "Configuration design in scalable reconfigurable manufacturing systems (RMS); A case of single-product flow line (SPFL)," *Int. J. Prod. Res.*, vol. 56, no. 11, pp. 3932–3954, Jun. 2018.
[28] A. M. Deif and W. ElMaraghy, "Investigating optimal capacity scalability scheduling in a reconfigurable manufacturing system," *Int. J. Adv. Manuf. Technol.*, vol. 32, nos. 5–6, pp. 557–562, Mar. 2007.
[29] F. Makssoud, O. Battaïa, and A. Dolgui, "Reconfiguration of machining transfer lines," in *Service Orientation in Holonic and Multi Agent Manufacturing and Robotics* (Studies in Computational Intelligence), vol. 472, 1st ed., T. Borangiu, A. Thomas, and D. Trentesaux, Eds. Berlin, Germany: Springer-Verlag, 2013, pp. 339–353, doi: 10.1007/978-3-642-35852-4_22.
[30] P. A. Borisovsky, X. Delorme, and A. Dolgui, "Genetic algorithm for balancing reconfigurable machining lines," *Comput. Ind. Eng.*, vol. 66, no. 3, pp. 541–547, Nov. 2013.
[31] K. K. Goyal and P. K. Jain, "Design of reconfigurable flow lines using MOPSO and maximum deviation theory," *Int. J. Adv. Manuf. Technol.*, vol. 84, nos. 5–8, pp. 1587–1600, Sep. 2015.
[32] A. Khezri, H. H. Benderbal, and L. Benyoucef, "Towards a sustainable reconfigurable manufacturing system (SRMS): Multi-objective based approaches for process plan generation problem," *Int. J. Prod. Res.*, vol. 59, no. 15, pp. 4533–4558, May 2020.
[33] L. K. Saxena and P. K. Jain, "A model and optimisation approach for reconfigurable manufacturing system configuration design," *Int. J. Prod. Res.*, vol. 50, no. 12, pp. 3359–3381, Jun. 2012.
[34] S. K. Moghaddam, M. Houshmand, K. Saitou, and O. F. Valilai, "Configuration design of scalable reconfigurable manufacturing systems for part family," *Int. J. Prod. Res.*, vol. 58, no. 10, pp. 2974–2996, May 2020.
[35] M. Bortolini, F. G. Galizia, C. Mora, and F. Pilati, "Reconfigurability in cellular manufacturing systems: A design model and multi-scenario analysis," *Int. J. Adv. Manuf. Technol.*, vol. 104, nos. 9–12, pp. 4387–4397, Oct. 2019.
[36] F. Hasan, P. K. Jain, and D. Kumar, "Optimum configuration selection in reconfigurable manufacturing system involving multiple part families," *OPSEARCH*, vol. 51, no. 2, pp. 297–311, Jun. 2014.
[37] F. Musharavati, N. Ismail, A. M. S. Hamouda, and A. R. Ramli, "A metaheuristic approach to manufacturing process planning in reconfigurable manufacturing systems," *Jurnal Teknologi*, vol. 48, no. 1, pp. 55–70, Jan. 2012, doi: 10.11113/jt.v48.219.
[38] A. Chaube, L. Benyoucef, and M. K. Tiwari, "An adapted NSGA-2 algorithm based dynamic process plan generation for a reconfigurable manufacturing system," *J. Intell. Manuf.*, vol. 23, no. 4, pp. 1141–1155, Aug. 2012.
[39] A. Bensmaine, M. Dahane, and L. Benyoucef, "Simulation-based NSGA-II approach for multi-unit process plans generation in reconfigurable manufacturing system," in *Proc. ETFA*, Sep. 2011, pp. 1–8.
[40] F. A. Touzout and L. Benyoucef, "Sustainable multi-unit process plan generation in a reconfigurable manufacturing environment: A comparative study of three hybrid-meta-heuristics," in *Proc. IEEE 23rd Int. Conf. Emerg. Technol. Factory Automat. (ETFA)*, Sep. 2018, pp. 661–668.
[41] Y. Koren, *The Global Manufacturing Revolution: Product-Process-Business Integration and Reconfigurable Systems*, vol. 80. Hoboken, NJ, USA: Wiley, 2010.
[42] H.-P. Wiendahl, H. A. ElMaraghy, P. Nyhuis, M. F. Zäh, H.-H. Wiendahl, N. Duffie, and M. Brieke, "Changeable Manufacturing–classification, design and operation," *CIRP Ann.*, vol. 56, no. 2, pp. 783–809, 2007.
[43] *A Modular Future How to Make Customization a Success—Buscar Con Google*. Munich, Germany: Roland Berger, 2019.
[44] P. Grznár, M. Gregor, M. Krajčovič, Š. Mozol, M. Schickerle, V. Vavrík, L. Ďurica, M. Marschall, and T. Bielik, "Modeling and simulation of processes in a factory of the future," *Appl. Sci.*, vol. 10, no. 13, p. 4503, Jun. 2020.
[45] K. Deb, A. Pratap, S. Agarwal, and T. Meyarivan, "A fast and elitist multiobjective genetic algorithm: NSGA-II," *IEEE Trans. Evol. Comput.*, vol. 6, no. 2, pp. 182–197, Apr. 2002.
[46] S. Lidberg, T. Aslam, L. Pehrsson, and A. H. C. Ng, "Optimizing real-world factory flows using aggregated discrete event simulation modelling: Creating decision-support through simulation-based optimization and knowledge-extraction," *Flexible Services Manuf. J.*, vol. 32, no. 4, pp. 888–912, Dec. 2020.
[47] A. H. C. Ng, J. Bernedixen, and A. Syberfeldt, "A comparative study of production control mechanisms using simulation-based multi-objective optimisation A comparative study of production control mechanisms using simulation-based multi-objective optimisation," *Int. J. Prod. Res.*, vol. 50, no. 2, pp. 359–377, Jan. 2012.
[48] W. M. Spears and K. D. De Jong, "On the virtues of parameterized uniform crossover," Nav. Res. Lab, Washington, DC, USA, Tech. Rep., Jan. 1995.
[49] A. H. C. Ng, J. Bernedixen, M. U. Moris, and M. Jagstam, "Factory flow design and analysis using Internet-enabled simulation-based optimization and automatic model generation," in *Proc. Winter Simul. Conf. (WSC)*, Dec. 2011, pp. 2181–2193.
[50] S. Bandaru, A. H. C. Ng, and K. Deb, "Data mining methods for knowledge discovery in multi-objective optimization: Part A–survey," *Expert Syst. Appl.*, vol. 70, pp. 139–159, Mar. 2017.

**CARLOS ALBERTO BARRERA DIAZ** received the B.Sc. degree in electrical engineering from the University of Malaga, Spain, and the B.Sc. degree in automation engineering and the master's degree in industrial systems engineering from the University of Skövde, Sweden, where he is currently pursuing the Ph.D. degree with the Intelligent Production Systems Division.

His research interests include design, modeling, simulation, and multi-objective optimization for the analysis of manufacturing systems.

**TEHSEEN ASLAM** received the Ph.D. degree in industrial informatics.

He is currently a Senior Lecturer at the University of Skövde, Sweden. His research interests include modeling, simulation, and multi-objective optimization for the design and analysis of supply chains.

**AMOS H. C. NG** is currently a Professor with the Division of Intelligent Production Systems, University of Skövde, Sweden. He is also a Visiting Professor with the Division of Industrial Engineering and Management, Uppsala University, Sweden, and the CEO of Evoma AB. His research interests include the applications of simulation, multi-objective optimization, and artificial intelligence in production/health-care/business systems.